



ELSEVIER

Earth and Planetary Science Letters 157 (1998) 193–207

EPSL

Water, partial melting and the origin of the seismic low velocity and high attenuation zone in the upper mantle

Shun-ichiro Karato *, Haemyeong Jung

Department of Geology and Geophysics, University of Minnesota, Minneapolis, MN 55455, USA

Received 17 March 1997; revised version received 29 December 1997; accepted 30 January 1998

Abstract

The common belief that the seismic low velocity and high attenuation zone (the asthenosphere) is caused by the presence of a small amount of melt is not supported by recent mineral physics and seismological observations. A review of recent mineral physics observations suggests that water significantly reduces seismic wave velocities through anelastic relaxation and hence, at a small melt fraction expected in most of the Earth's upper mantle, partial melting will *increase* seismic wave velocities through the removal of water from minerals such as olivine. Therefore the asthenosphere, in this model, is a layer where *no* significant partial melting occurs and hence a high water content is retained. We apply this model to calculate seismic wave velocities and attenuation in the upper mantle with a range of water contents. The seismic structures calculated from this model depend on geotherm, the mode of partial melting (batch or fractional melting) and the geometry of upwelling flow (passive flow or dynamic upwelling). The sharp velocity change around 60–80 km (the Gutenberg discontinuity) can be attributed to a sharp change in water content due to partial melting, if the temperature there is relatively high as implied by the plate model and if melting occurs as fractional melting but not by batch melting. However, the significant increase in seismic wave velocity with age in young oceanic upper mantle suggests rapid cooling as predicted by a cooling half-space model. Thus, the present model suggests fast cooling in the early stage but slow cooling in the later stage of evolution of the oceanic upper mantle, the latter being caused presumably by some additional heat in the old oceanic upper mantle. The seismic structures of typical oceanic upper mantle with a fast spreading rate (e.g., the Pacific) is consistent with passive spreading, whereas the greater depth of the G-discontinuity and the weaker seismic anisotropy in back-arc regions (e.g., the Philippine Sea) suggest dynamic upwelling caused presumably by a higher degree of melting due to a larger amount of water. © 1998 Elsevier Science B.V. All rights reserved.

Keywords: lithosphere; asthenosphere; water; partial melting; anelasticity

1. Introduction

It has long been believed that most of the geophysical anomalies of the asthenosphere, namely low velocities and high attenuation of seismic waves,

high electrical conductivity and low viscosity [1,2], are due to the presence of a small amount of melt [3,4]. However, many experimental studies on the effects of partial melting of peridotites have failed to demonstrate significant effects of partial melting on these physical properties for a range of melt fractions expected over most upper mantle conditions (say 1–3% or less). For example, it has been shown

* Corresponding author. Fax: 612-625-3819; E-mail: karato@maroon.tc.umn.edu

that when a small amount of basaltic melt is added to dry (water-free) olivine-rich aggregates, only a minor enhancement of deformation is observed (for a review, see [5]). This is mainly a result of the fact that basaltic melt does not wet grain-boundaries of peridotites. For the same reason, the direct effects of partial melting on seismic wave velocities at a small melt fraction are also small [6,7].

However, the effects of water on various physical properties, particularly those that are related to defect motion, are dramatic [8,9]. Based on these two observations and also on the well known fact that water can be dissolved in melts much more than in solid minerals [10,11], Karato [12] proposed that the main effect of partial melting might be the removal of water from solid minerals and hence to increase the creep strength and to affect other related properties. Hirth and Kohlstedt [13] further developed this model to investigate the rheological structure of oceanic upper mantle and suggested that rheological stratification of the oceanic upper mantle into lithosphere and asthenosphere might be largely due to the stratification in intragranular water content. Although these studies provided a new perspective for the rheological stratification of the Earth's upper mantle, observational tests of the model are difficult because the resolution of estimation of rheological stratification is limited.

In contrast, much more detailed information can be obtained on the seismic structure of the upper mantle and therefore it is desirable to extend such a model to explore its seismological consequences. By comparing model predictions with observations, better constraints on the structure and properties of the Earth's upper mantle will be obtained. The purpose of this paper is thus to explore some implications of this 'drying out' model for the seismic structure of the upper mantle of the Earth. The key observations that we would like to explain are: (1) a sharp decrease in seismic wave (particularly shear wave) velocities at the Gutenberg (G)-discontinuity (at 60–80 km depth), and (2) a peculiar regional variation of the depth of the G-discontinuity: the depth of the G-discontinuity in back-arc regions is deeper than that in the western Pacific in contrast to expectations from the ages of oceanic lithosphere in these regions [14,15]. We will first show that these observations are difficult to explain with conventional models. We

will then propose a new model in which the anelastic relaxation enhanced by water [16] plays a key role in determining the seismic velocity versus depth profile in the upper mantle. It will be shown that both of the two features can be attributed to the depth and regional variation of water content in the upper mantle. Our model also provides a natural explanation for the regional variation of seismic anisotropy. We will finally summarize some predictions of the present model that can be tested either experimentally or seismologically.

2. Difficulties with previous models of the low velocity zone

Previous models of the low velocity and high attenuation zone assume either that (1) these anomalies are due to the presence of a small amount of melt [3,4], or that (2) they are due to enhanced anelasticity due to high temperatures [17,18]. The first model is based on the experimental observation on the NaCl–H₂O system [19] in which the onset of partial melting results in a sharp decrease in elastic wave velocity. This model can explain the observed sharp change in seismic wave velocity at the lithosphere–asthenosphere boundary [14,15], but is inconsistent with the experimental observation that a small amount of melt in peridotites does not significantly reduce seismic wave velocities [7]. The difference in the effects of partial melting on seismic wave velocities between upper mantle rocks and NaCl–H₂O is due to the difference in wetting behavior: in upper mantle rocks melt does not wet grain-boundaries [5], but in NaCl–H₂O it does [19]. Therefore although the presence of partial melt may explain low velocities in regions near mid-ocean ridges, this model fails to explain the presence of a low velocity zone in old oceanic upper mantle. Furthermore, this model cannot explain the observed greater depth of the G-discontinuity in the upper mantle of back-arc regions compared to the old Pacific upper mantle [14,15]: the model predicts that G-discontinuity should be shallower in the back-arc regions (Fig. 1).

An alternative model assumes that the low velocity is due to significant anelasticity due to high temperatures [17,18]. This model provides a mechanism

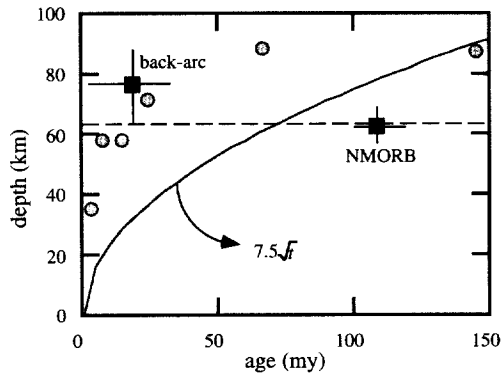


Fig. 1. The relation between the depth (d) of the lithosphere–asthenosphere boundary and the age (t) of oceanic upper mantle. The solid line is based on the Rayleigh wave dispersion [21], showing $d \sim \sqrt{t}$ in which inversion was made assuming isotropic structure. The solid circles are the results of Forsyth [22] in which SH/SV polarization anisotropy was included in the inversion. The solid squares are the results of the ScS reverberation analysis by Revenaugh and Jordan [15] and Gaherty et al. [14]. The latter technique detects a sharp discontinuity, whereas the surface wave techniques are insensitive to a (small) discontinuity. Previous models for the low velocity zone predict that the depth of the lithosphere–asthenosphere boundary increases with age approximately following a $d \sim \sqrt{t}$ relation. Note that the reverberation technique shows that the depth of the G-discontinuity does not change with age, but its depth in back-arc regions is somewhat deeper than those in the typical oceanic upper mantle (NMORB source regions).

for low velocities and high attenuation in regions where no significant partial melting is expected. However, this model fails to explain the observed regional variation in the depth of the G-discontinuity; this model also predicts that the G-discontinuity should be shallower in the back-arc regions than in the normal mid-ocean ridge basalt (NMORB) source regions. Furthermore, since the change in anelasticity with temperature is gradual in this model, it is difficult to explain the sharp discontinuity inferred from S-wave reverberation studies [14,15].

3. Water-enhanced anelasticity and its effect on seismic wave velocities

The above analysis suggests that an alternative model is necessary to explain the origin of the seismic low velocity and high attenuation zone. We propose that the sharp reduction in seismic wave

velocity at the G-discontinuity is due to a sharp increase in intragranular water content due to partial melting. This model is based on two notions proposed before: (1) water enhances anelastic relaxation [16], and (2) the main role of partial melting in affecting physical properties is through the removal of water from solid minerals such as olivine [12]. In what follows, these two notions will be quantified with a use of realistic models of the oceanic upper mantle.

For a given bulk chemistry of the upper mantle, major factors that control the seismic wave velocities are temperature and pressure. The seismic wave velocities are also likely to be sensitive to water content (or water fugacity) through its effect on anelasticity [16]. When the effects of both anharmonicity and anelasticity are considered, the effects of temperature (T), pressure (P) and chemical environment (C) on seismic wave velocity (V) can be written as [18]:

$$V(\omega, T, P, C) =$$

$$V_0(T, P) \left[1 - \frac{1}{2} \cot\left(\frac{\pi\alpha}{2}\right) Q^{-1}(\omega, T, P, C) \right] \quad (1)$$

where $V_0(T, P)$ is the seismic wave velocity as a function of temperature and pressure when only anharmonic effects are important. This part of the T – P dependence is nearly independent of frequency and of chemical environment and can be measured by high frequency laboratory experiments such as ultrasonic measurements [23] or Brillouin scattering [24]. The second term in Eq. 1 represents the effects of anelastic relaxation where $Q^{-1}(\omega, T, P, C)$ is seismic wave attenuation which is a function of frequency (ω) and T, P and parameters (C) that specifies the chemical environment (such as water fugacity). Both laboratory measurements and seismological observations suggest [25]:

$$Q^{-1} \sim \omega^{-\alpha} \quad (2)$$

with $\alpha = 0.1$ – 0.3 . Using microscopic models of anelasticity, this relation implies [25]:

$$Q^{-1} \sim (M/\omega)^\alpha \quad (3)$$

where M is the mobility of defects such as dislocations. M can be written as:

$$M = M_0 \exp\left(-\beta \frac{T_m(P)}{T}\right) \quad (4)$$

where T_m is the melting temperature of the mineral that depends on pressure (P) and β is a non-dimensional parameter related to the activation enthalpy (H^*) as $H^* = \beta RT_m$.

In many silicates, the mobility of defects including point defects, dislocations and grain-boundaries depends also on water content (C_{OH}) [26]. As a first approximation, we assume that the mobility of defects is linearly proportional to the water content [13,27]. Thus,

$$Q^{-1} = \left[\frac{(A + BC_{OH})}{\omega} \right]^\alpha \exp\left(-\alpha\beta \frac{T_m}{T}\right) \quad (5)$$

where A (B) is a parameter related to anelasticity at dry (wet) conditions. There have been no systematic experimental studies of the effects of water on Q . However, analysis of the existing data on Q [7,28] as well as theoretical considerations strongly suggest that water should enhance anelasticity. In fact, Jackson et al. [28] found that dunite specimens that were pre-dried at 1473 K showed significantly smaller attenuation (they observed that Q is a factor of 2–3 larger than in *as-is* specimens which contain a significant amount of water). The results are consistent with the above model, because creep rate (dislocation mobility) is enhanced by the presence of water by ~ 100 under these conditions, which implies a factor of $\sim (100)^\alpha$ increase in Q upon drying, if a dislocation mechanism of attenuation is assumed [25,28]. With $\alpha \sim 0.2$ [28], this yields a factor of ~ 2.5 increase in Q , which is consistent with the experimental observation.

In evaluating the effects of anelasticity in the upper mantle, we used the activation energy and the frequency dependence of Q and melting temperatures determined by laboratory experiments [28,29], but we used parameters A and B constrained by seismological observations [30]. The reason is because laboratory results on natural specimens may not be directly applicable to the Earth's interior because of the difference in dislocation density. The sample used in Jackson et al. [28] is a natural dunite from Aheim, Norway, which has a dislocation density of $\sim 10^{11} \text{ m}^{-2}$. Dislocation densities in the Earth's upper mantle may be much less, which will cause a difference in pre-exponential factors (A and B) but not the activation energy nor the frequency dependence (α). To determine the parameters A and B , we

Table 1

Parameters for seismic wave attenuation: $\beta = 25$

Frequency dependence	A ($= B$) (Hz)
<i>Plate model</i>	
$\alpha = 0.1$	2.4×10^{-7}
$\alpha = 0.2$	6.7×10^2
$\alpha = 0.3$	9.0×10^5
<i>Cooling half-space model</i>	
$\alpha = 0.1$	7.3×10^{-6}
$\alpha = 0.2$	9.7×10^3
$\alpha = 0.3$	8.8×10^6

The functional form of $Q^{-1}[(A + BC_{OH})/(\omega)]^\alpha \exp[-\alpha\beta(T_m)/T]$ is assumed (Eqs. 1 and 5).

shall further make two assumptions: (1) the average Q in the asthenosphere (depth from 60 to 220 km) is $Q = 80$ ([30]) and (2) Q at water-free conditions and at water-rich conditions become comparable when $C_{OH} = 1$ ppm H/Si. The latter assumption is equivalent to the assumption that the addition of ~ 100 ppm H/Si of water enhances dislocation mobility by a factor of ~ 100 [13]. The A and B thus estimated are shown in Table 1 together with the parameters β and α . These parameters predict slightly higher Q values under asthenospheric conditions than the values estimated from the laboratory data on Aheim dunite [28] ($Q = 20$ – 40 is predicted when the results of Jackson et al. [28] are directly extrapolated to the likely conditions of the asthenosphere). This discrepancy may be due to the difference in dislocation density between their specimens and the Earth's mantle.

4. Geotherm, partial melting and water in the upper mantle

4.1. Composition of the upper mantle

The chemical composition of major elements of MORBs (Mid-Ocean Ridge Basalts) is remarkably homogeneous [4], although significant differences are observed in the chemistry of highly incompatible elements including water [31–34]. Therefore, in considering the seismic structure of the upper mantle, we assume that major element chemistry is homogeneous and does not vary laterally among the source regions of MORB. A typical source material for the

MORB is pyrolite which contains ~50–60% olivine, ~20–30% orthopyroxene, ~10–20% clinopyroxene and ~5–10% garnet or spinel [4]. Because physical properties such as the temperature and pressure derivatives of seismic wave velocities and seismic wave attenuation are well constrained only for olivine, we use a crude approximation that properties of other minerals are similar to those of olivine. Under this assumption, a mineralogical transition such as from spinel lherzolite to garnet lherzolite has no significant effects on seismic wave velocities [35]. However, large lateral and radial variations in water content are expected in the upper mantle, and these will affect the seismic wave velocity significantly [16]. Therefore, we consider the variation of seismic wave velocities caused by a change in temperature (T), and pressure (P) and water content. We assume that the water content in the source region of MORB varies from one place to another, and we will consider two cases: NMORB source region such as the Pacific and a back-arc MORB source region such as the Philippine Sea. The water content in the former is assumed to be 0.01 wt% and in the latter 0.04 wt% [34]. For a given water content in the source region of MORB, the vertical variation in water content is calculated following the procedure described in Section 3.

4.2. Geotherm

Two models of oceanic geotherms will be considered (Fig. 2). One is a cooling half-space model [36] and the other is a plate model [37]. In both models, the geotherm is a function of the age of the oceanic lithosphere. We calculate velocity and attenuation profiles for several ages. Parameters in both models are chosen to fit various geophysical observations including the surface heat flow and ocean floor bathymetry. In the plate model, the thickness of the mechanical plate is assumed to be 60 km, which is consistent with the rheological model of Hirth and Kohlstedt [13]. We used McKenzie and Bickle's [38] model to calculate the temperature distribution in the thermal boundary layer beneath the mechanical boundary layer. We use the viscosity of $\sim 10^{18}$ Pa s based on Hirth and Kohlstedt [13]. With this viscosity, the thickness of the thermal boundary layer is ~ 75 km. The two models yield similar temperature profiles near the surface in relatively young

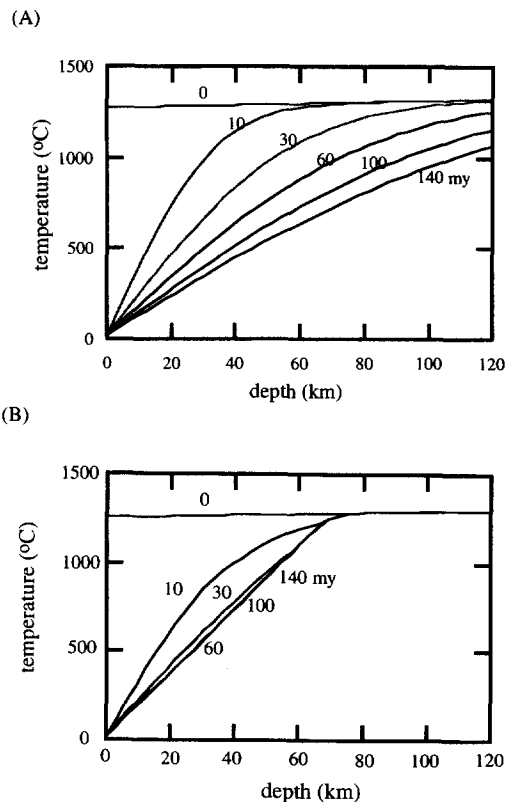


Fig. 2. Geotherms of the upper mantle for various ages. (A) Cooling half-space model [36]. (B) Plate model. For the plate model [37], we assumed the thickness of the plate (the mechanical boundary layer) is 60 km and the temperature at the boundary is 1373 K. The temperature beneath the plate is calculated using the model by McKenzie and Bickle [38].

age (< 10 Ma) but the temperature profile in the deep lithosphere and asthenosphere for older ages is markedly different. The plate model gives significantly higher temperatures in the deep portions and the temperature profiles do not change significantly with age for ages larger than ~ 30 Ma.

4.3. Partial melting and depletion of water from olivine

When materials in the source region ascend and partial melting occurs, water will be depleted from minerals because basaltic melt has much higher solubility of water than minerals [12]. Upwelling peridotites will melt at a certain depth when the solidus is exceeded. The melting of peridotites with a small

amount of volatiles will occur with two distinct stages [32]: partial melting starts when the solidus of 'wet' peridotite is exceeded, but the amount of melt produced is controlled by the amount of water. The initial depth of melting and the melting behavior under water-present conditions depend on the water content. The depth at which partial melting initiates is estimated from the solidus using a method similar to that of Hirth and Kohlstedt [13], but we use the activity of water in melt rather than that in olivine to estimate the melting relation. We find that melting starts at ~ 160 km in the NMORB source regions, whereas it starts at ~ 250 km in the source region of back-arc type MORB. The melt fraction in this water-assisted melting regime is assumed to be a linear function of depth and is up to $\sim 0.25\%$ for a NMORB source region and up to $\sim 1\%$ for a back-arc MORB source region [33,40,41]. When the 'dry' solidus is exceeded (at ~ 65 km), then much more significant partial melting occurs. The rate of melting at this stage is $\sim 0.3\%/km$ [41].

Since upper mantle peridotite is usually undersaturated with water, partial melting will cause depletion of water from minerals [12]. The manner in which water is removed from solid minerals depends on the process of melting. It is effective if melt is removed from the system immediately after melting (fractional melting) but is less effective if melt remains in chemical equilibrium throughout the melting process (batch melting). Based on geochemical observations [33,39] and melt permeability measurements [5], we assume fractional melting in this paper. We use the relation of Shaw [42] to estimate the water content as a function of depth (see also [13]). The results are shown in Fig. 3. Note that water content in olivine gradually decreases as depth decreases and when the dry solidus is reached there is a sharp decrease in water content because of a much higher degree of melting.

4.4. Mode of upwelling flow beneath mid-ocean ridges

The actual water content versus depth relation in a peridotite column away from the ridge is determined by the water content of the peridotite at the time water content is frozen and the geometry of flow after this time. Since solid state diffusion is slow

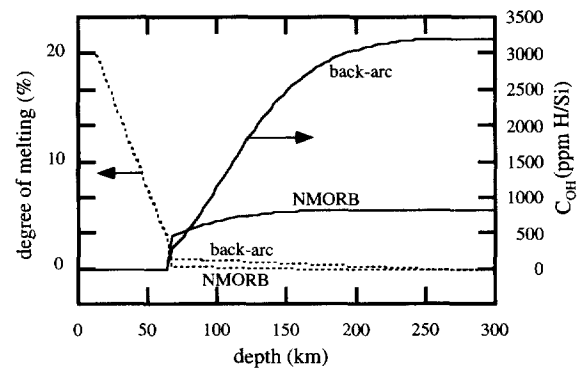


Fig. 3. Water content (C_{OH}) in olivine (solid curves) and degree of melting (broken curves) as a function of depth beneath a mid-ocean ridge corresponding to two different water contents in the source region (a source region for NMORB and source region for back-arc MORB). The water content in olivine decreases when partial melting occurs due to selective partitioning of water into melt [12,13]. Melting starts at a depth at which the geotherm intersects the solidus for a given water content. The depletion of water is moderate in the deep regions where water-assisted melting occurs. Much more significant water depletion occurs when the dry solidus is exceeded (at around 65 km).

even at a geological time scale, we assume that once partial melting terminates, no significant transfer of water occurs. Assuming fractional melting, the water content of a rock can be considered to be effectively fixed when the maximum degree of melting (along a certain path) is reached. After the water content is fixed, a piece of peridotite will flow before it is incorporated into a rigid plate. The flow line that a piece of peridotite will follow depends on the mechanism of flow [41]. For example, for passive flow, the water content in a peridotite column at a given depth will be similar to the water content at the same depth beneath a mid-ocean ridge. On the other hand, if dynamic flow occurs, the water content of a peridotite column will reflect the water content at much shallower depth [41]. In dynamic flow, the exact profile of water content versus depth depends on the flow pattern which is sensitive to the magnitude and spatial distribution of buoyancy forces as well as rheological profiles [43] and cannot be precisely specified. However, the general tendency is that flow lines are more compressed in the deep lithosphere and hence that the velocity change at the G-discontinuity becomes sharper and the depth of the G-discontinuity tends to be greater (Fig. 4).

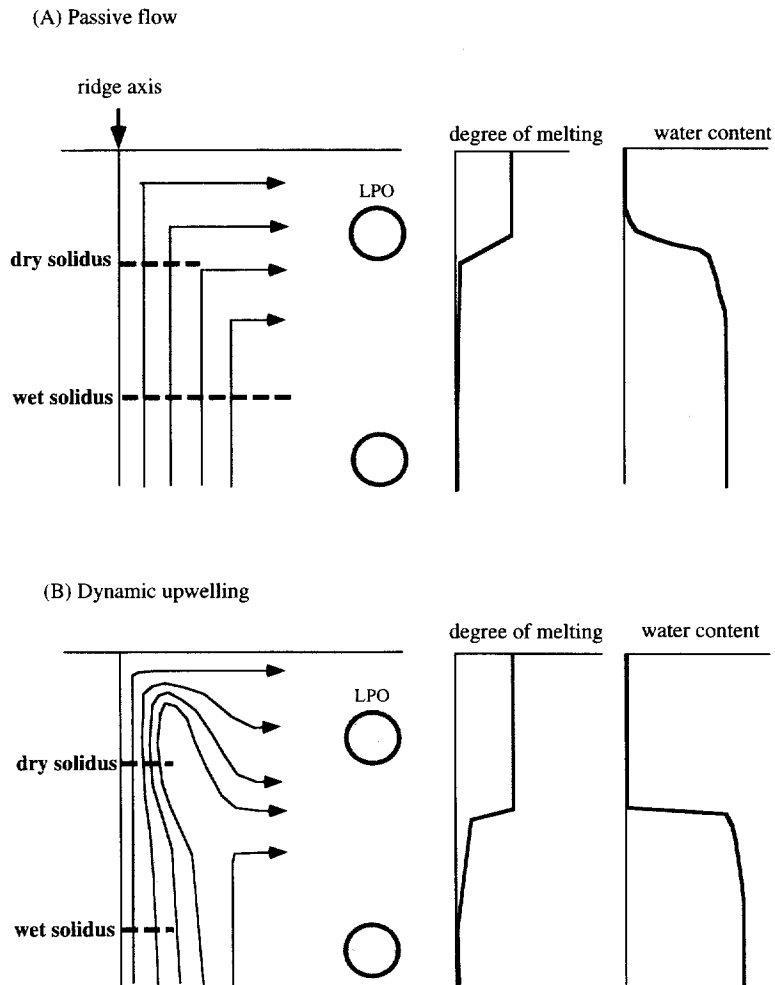


Fig. 4. Schematic diagrams illustrating partial melting and the flow pattern beneath a mid-ocean ridge corresponding to (A) passive flow and (B) dynamic (buoyancy-driven) flow. The degree of melt depletion and associated water content in a residual mantle column are shown schematically. The degree of melting increases rapidly once the dry solidus is exceeded and therefore the water content changes significantly at that depth. The water content versus depth profiles depend also on the geometry of flow. Water content changes with depth more sharply for dynamic flow than passive flow. The LPO (lattice preferred orientation) of olivine in a residual peridotite column (schematic) is based on a model of the flow pattern by Blackman et al. [44] and experimental results on LPO by Zhang and Karato [45], and the bar shows the orientation of a -axes of olivine. Less azimuthal anisotropy is expected in the lithosphere in the dynamic upwelling regime than in the passive flow regime, although the nature of anisotropy will be similar in the asthenosphere where flow is nearly horizontal in both cases. Dynamic upwelling is likely to be caused by a larger degree of partial melting at deeper portions and hence the thickness of the lithosphere will be larger where dynamic upwelling occurs.

According to Scott and Stevenson [43], the dynamic upwelling due to buoyancy forces becomes important if the following relation is satisfied,

$$\frac{0.1 \cdot x^2 \cdot g \cdot \Delta\rho \cdot \phi}{\eta} > v_L \quad (6)$$

where x is the width of the upwelling current (~ 30 km), g the acceleration due to gravity, $\Delta\rho$ the density difference between melt and solid (~ 500 kg/m³), ϕ the melt fraction, η the viscosity and v_L the spreading rate. Fig. 5 shows the viscosity–melt fraction diagram to show dominant mode of upwelling flow

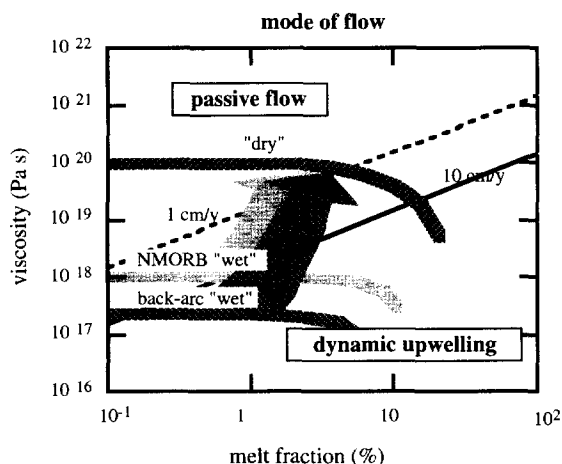


Fig. 5. Mechanisms of upwelling as a function of viscosity and melt fraction (Eq. 6 in the text based on Scott and Stevenson [43] is used and the width of upwelling is assumed to be 30 km). Dynamic flow dominates at low viscosity, large melt fraction and slow spreading rate. Viscosity of upwelling materials is dependent upon degree of melting through the effects of water depletion [12,13] and also on melt fraction [55]. Because of high permeability of basaltic melt in olivine-rich rocks [5], melt fraction over the most of upper mantle conditions is expected to be small (<1–2%). At the initial stage of melting, both the degree of melting and melt fraction are small and the peridotite will assume 'wet' rheology without much effects of partial melting. Upon increasing the degree of melting, rheology will change from 'wet' to 'dry' due to a 'drying out' effect as indicated by arrows [12,13]. It is seen that dynamic upwelling is unlikely to occur in NMORB source regions with a fast spreading rate (e.g., the Pacific upper mantle) whereas it may occur in most back-arc regions and NMORB source regions with a slow spreading rate.

near mid-ocean ridges together with the relations between viscosity and melt fraction estimated from the model by Karato [12] and Hirth and Kohlstedt [13]. In order to satisfy the condition for dynamic upwelling, one needs to have a significant amount of melt where the viscosity of partially molten materials is low. This is a difficult condition to be met in NMORB source regions, but may be met in some portions of back-arc regions (Fig. 5). We conclude therefore that, in back-arc upper mantle where a significant amount of water is present, dynamic upwelling may occur over a wide range of conditions, whereas in the source region of NMORB dynamic upwelling is limited to very slow spreading centers (e.g., Atlantic).

5. Seismic structure of the lithosphere–asthenosphere

We have calculated seismic wave (shear wave) velocities and attenuation based on the model. The frequency is assumed to be 1 Hz. We used two geotherms (cooling half-space model and plate model) and calculated velocities and attenuation for several ages. For water content–depth profiles, we consider a NMORB source region (water content is 0.01 wt%) and a back-arc region (water content is 0.04 wt%). We also consider the water content–depth profiles corresponding to passive flow and dynamic upwelling.

The results are shown in Fig. 6 and can be summarized as follows:

(1) A sharp discontinuity in velocity can occur at ~65 km because of a sharp change in water content, if temperature there exceeds ~1000°C (Fig. 6A–D). The sharpness depends somewhat on the flow pattern: dynamic flow predicts a sharper velocity change (Fig. 6F).

(2) The depth of the G-discontinuity does not change with the age of the lithosphere (Fig. 6D).

(3) The water content in the source region does not have direct effects on the depth of the G-discontinuity (Fig. 6E), although the difference in water content may cause some indirect effects, through changes in the depth of water-assisted melting and through the difference in the amount of melts that may affect the dynamics of upwelling (see Section 6).

(4) The velocities of seismic waves increase significantly with the age of oceanic lithosphere if the cooling half-space model is assumed (Fig. 6D). In contrast, the age dependence is much less in the plate model (Fig. 6D).

(5) The frequency dependence of anelasticity has some effects. When frequency dependence is strong, the effective activation energy becomes larger and hence attenuation in the shallower portions becomes less important (Fig. 6C).

6. Discussion

6.1. Temperatures in the upper mantle

The present model can explain some of the seismological observations on the upper mantle,

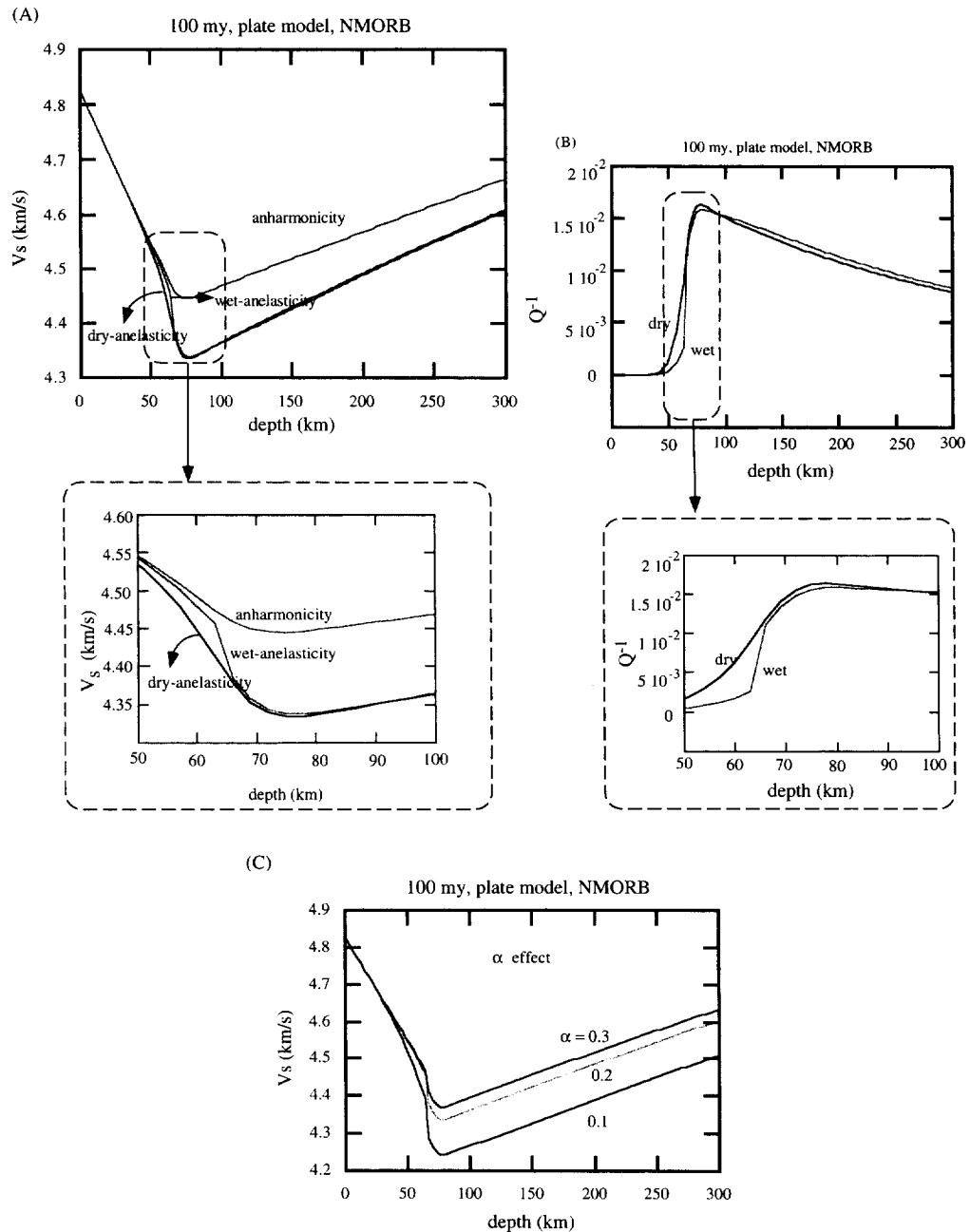


Fig. 6. Calculated seismic wave velocities (and attenuation) in the upper mantle. (A) Effects of mechanisms to control seismic wave velocities. Comparison of various effects including anharmonicity, anelasticity without the effects of water (dry-anelasticity) and anelasticity with the effect of water (wet-anelasticity) for a plate model geotherm at 100 Ma old NMORB source region. It is seen that a sharp change in water content is necessary to explain the sharp change in velocities at the G-discontinuity observed by Revenaugh and Jordan [15] and Gaherty et al. [14]. (B) Seismic wave attenuation as a function of depth corresponding to the velocity profiles shown in (A). Both 'wet' and 'dry' cases are shown. (C) Effects of frequency dependence. Numbers are the parameter α that characterizes the frequency dependence of attenuation (see Eq. 2). Geotherm corresponding to a plate model (for 100 Ma) is assumed.

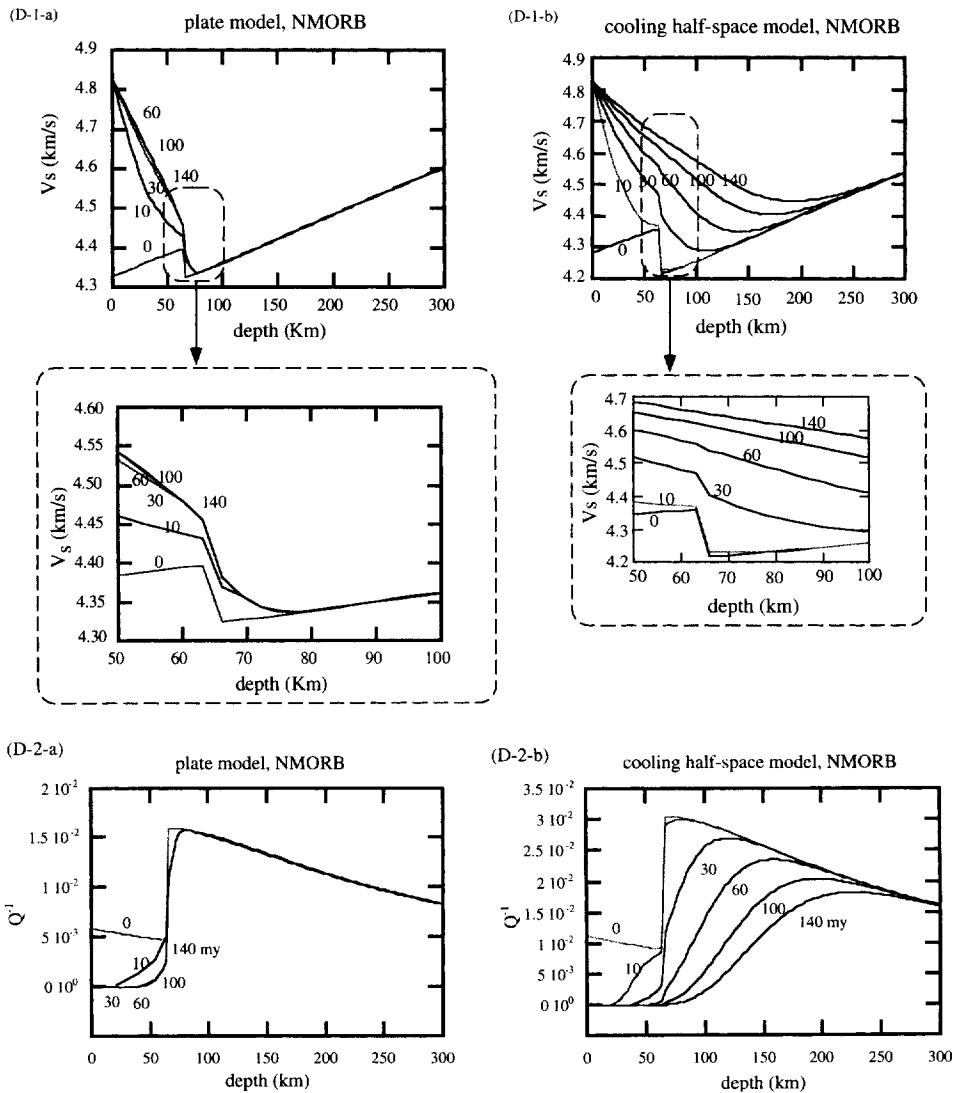


Fig. 6 (continued). (D) Effects of geotherm and age. Seismic wave velocity (D-1) and attenuation (D-2) versus depth relations for two different geotherms. The effects of water are included.

particularly the nature of the G-discontinuity (the lithosphere–asthenosphere boundary). Our results suggest that the temperatures in the deep lithosphere in old oceanic mantle must be significantly higher than the simple cooling half-space model predicts. A geotherm corresponding to the cooling half-space model predicts $T \sim 800^\circ\text{C}$ at this depth (Fig. 2) and the effects of anelastic relaxation are negligible (Fig. 6D). Therefore this model can be rejected for old oceanic upper mantle if the G-discontinuity is to

be attributed to enhanced anelasticity due to water.

However, the plate model predicts a very small age dependence of seismic wave velocities (Fig. 6D). This is not consistent with the results of surface wave studies (e.g., [2,22]) which indicate a significant increase in velocities with age, particularly at relatively young ages. We conclude therefore that a temperature profile corresponding to the cooling half-space model may apply to relatively young oceanic upper mantle, whereas a temperature profile corresponding

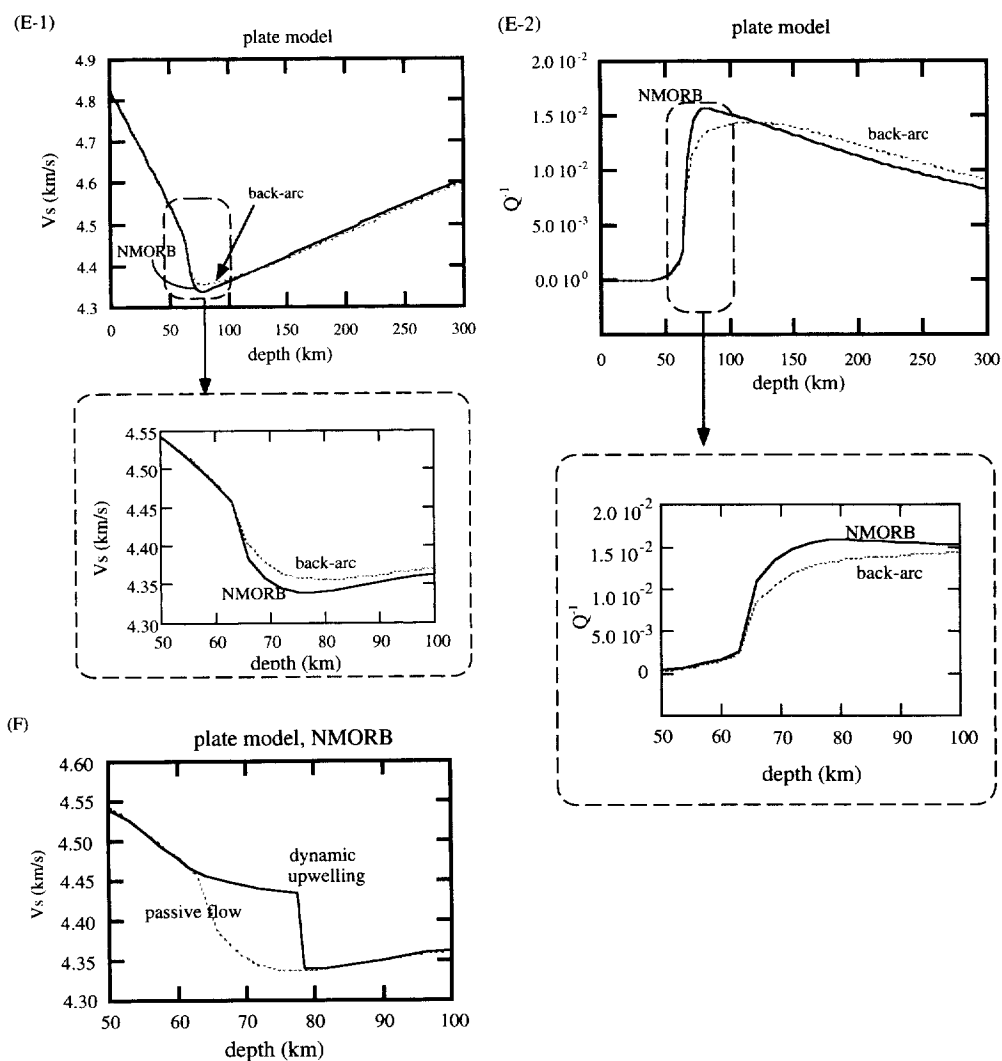


Fig. 6 (continued). (E) Effects of water content, (E-1): seismic wave velocity, (E-2) seismic wave attenuation. A comparison of models with two different water contents (source regions for NMORB and back-arc spreading), but otherwise identical conditions (100 Ma old and plate model geotherm). See Fig. 3 for the difference in water content versus depth curves between the two cases. (F) Effects of mode of flow. A comparison of the velocity–depth relation (at 100 Ma) for passive flow and dynamic flow. The relation for dynamic flow is schematic. The dynamic flow model predicts a sharper change in velocities at the lithosphere–asthenosphere boundary. A greater depth of the G-discontinuity is expected for the dynamic flow model than for the passive flow model due to the difference in flow geometry (see Fig. 4).

to the plate model better represents the geothermal gradients in old oceanic upper mantle. This means that the oceanic upper mantle cools rather rapidly when it is young, but much more slowly when it gets old. The presence of some excess heat source is therefore suggested from this analysis which is consistent with an earlier suggestion based primarily

on the analysis of ocean floor bathymetry and heat flow observations [46] and geoid anomalies [47].

6.2. Partial melting in the upper mantle

It is now well appreciated that significant partial melting in the upper mantle occurs only in the near

vicinity of mid-ocean ridges (e.g., [38]). Our model suggests that the partial melting that occurs near mid-ocean ridges controls the water content versus depth relation that in turn determines seismic wave velocities in the oceanic upper mantle away from ridges.

Our model indicates that partial melting has a significant effect on seismic wave velocities, but the effects are opposite to those what have been believed: we predict that partial melting will *increase* seismic wave velocities in most cases. Therefore the previous attempts at inferring partial melting in the upper mantle from seismic observations (e.g., [2]) must be re-evaluated. Partial melting will affect seismic wave velocities in two different ways. First, it will increase the average velocity as discussed above. The observed high velocity anomalies near the ridge crest, which were interpreted to be due to lattice preferred orientation [48], may be partly due to the effect of water depletion. Second, because partial melting in the Earth occurs where materials are dynamically deforming under stress, preferred orientation of melt shape will occur [49] that will cause seismic anisotropy [50]. These effects must be taken into account in the geodynamical interpretation of seismic wave velocity anomalies in the upper mantle.

It should also be noted that the change in seismic velocities associated with the depletion of water in a residual peridotite column will occur only when the mode of partial melting is fractional melting as opposed to batch melting. No depletion of water from minerals will occur in a peridotite column if melting occurs through strictly batch melting (unless separation of melt from solid occurs through dykes at shallower depths, which is effectively 'fractional melting').

6.3. Regional variation in the upper mantle seismic structures

Gaherty et al. [14] and Revenaugh and Jordan [15] showed some differences in the seismic structure between back-arc regions and the old Pacific oceanic upper mantle (Fig. 1). The G-discontinuity in the upper mantle of back-arc regions is deeper than that in the old Pacific and the velocity jump in the back-arc regions is smaller than that in the Pa-

cific. Likewise, Yu and Park [51] showed a marked difference in the nature of seismic anisotropy in the upper mantle of typical Pacific oceanic mantle and in the Philippine Sea upper mantle: anisotropy is significant in the Pacific, but not in the Philippine Sea upper mantle. Similarly, seismic anisotropy in the Atlantic upper mantle appears to be significantly less than that in the Pacific upper mantle [52,53].

These two observations may have a common cause: dynamic upwelling in the back-arc upper mantle and in NMORB sources with a slow spreading rate, and passive spreading in NMORB source regions with a fast spreading rate (see Figs. 4 and 5). A lower viscosity caused by a higher water content and/or a slower spreading rate will favor dynamic upwelling (Fig. 5). Dynamic upwelling tends to deepen the G-discontinuity and weaken the seismic anisotropy through its effect on the flow lines (see Fig. 4).

6.4. Comparison with laboratory studies

Sato et al. [7] made laboratory measurements of seismic wave velocities and attenuation of a peridotite in a temperature range spanning the solidus. Their results do not show any appreciable change in attenuation nor velocities upon partial melting. The experimental study by Berckhemer et al. [54] also included the temperature range of melting and did not show a sudden change in attenuation upon melting. How can these results be compared with the present model?

First, the results by Berckhemer et al. [54] are at room pressure and therefore water do not play any significant role because of low water fugacity. Second, Sato et al.'s [7] study was under high pressure, up to 0.7 GPa, and the role of water might be important. However, three issues make the interpretation of their results difficult. First, although the water content in their samples is likely to be significant (see [25]), no measurements were reported on the water content in their samples. Second, the 'drying out' effect proposed by Karato [12] applies only to the case where the system is undersaturated with water. It is not clear whether Sato et al.'s specimens were undersaturated with water or not. Third, the effects of water are likely to be through anelastic relaxation and hence are frequency-dependent. Sato et al.'s [7]

measurements were made at ~ 500 kHz and the attenuation at these frequencies is likely to be much less than that at low seismic frequencies. We consider therefore that Sato et al.'s [7] study measured the effects of anelasticity with higher characteristic times and hence the effects on seismic wave velocities which they obtained must be considered as a lower bound; any additional (low frequency) mechanisms would further reduce the velocities.

Are there no experimental observations to support the present model? Jackson et al.'s [28] results indicate a significant effect of water for enhancing anelasticity. In addition, a comparison of Sato et al.'s [7] results with others also suggests that water in Sato et al.'s specimens may have enhanced anelasticity [25]. Another point in our model is the extraction of water from minerals upon partial melting [12]. Such behavior has been demonstrated by Hirth and Kohlstedt [55] and similar effects have been inferred from the measurements of highly incompatible elements [20,31–33,41]. Therefore, experimental observations available support the model in general.

7. Concluding remarks

The present analysis has shown that water plays an important role in determining the distribution of seismic wave velocities as well as other physical properties such as viscosity [8,12,13] and electrical conductivity [9]. It appears that the most important effect of partial melting is not its direct effect on these properties as has been considered in most of the previous studies [1,2], but its indirect effect through the change in water content in solid minerals [12]. In this regard, one of the most important issues in mineral physics is to demonstrate the role of water on seismic wave attenuation by high pressure, high temperature and low frequency measurements [28].

It is also important to carry out seismological tests of the present model. A straightforward prediction of the model is that the depth of G-discontinuity is independent of age (t). This is different from the prediction of most previous models which predict $d \sim \sqrt{t}$ where d is the thickness of the oceanic lithosphere (the depth of the G-discontinuity). Therefore measurement of the depth of the G-discontinuity as a function of the age of oceanic lithosphere will pro-

vide the best test for the model (Fig. 1). It should be noted, however, that the present model is consistent with surface wave studies which show the growth of oceanic lithosphere following the $d \sim \sqrt{t}$ relation [21], because in surface wave studies one measures velocities of average upper mantle and does not see subtle velocity discontinuities. The average velocities of the oceanic upper mantle do change with age in this model (see Fig. 6).

Finally, we note that the depth of the G-discontinuity, in our model, corresponds to the depth at which seismic wave attenuation changes due to a change in water content. Therefore, the G-discontinuity corresponds *directly* to the depth at which a change in rheological properties occurs [13]. This is in marked contrast with previous models in which the relation between the seismic and the rheological lithosphere is indirect and hence the thicknesses estimated from the two definitions are very different (e.g., [18]).

Acknowledgements

SK thanks Jim Gaherty and Tom Jordan for discussions of seismological observations at MIT in the summer of 1995 that led to the present model, and Greg Hirth and Dave Kohlstedt for discussions on some mineral physics issues. Comments by Greg Hirth, Jan Tullis and an anonymous reviewer were helpful in improving the presentation of this paper. This research was supported by NSF grant OCEA-9529744. [RO]

References

- [1] T.J. Shankland, R.J. O'Connell, H.S. Waff, Geophysical constraints on partial melt in the upper mantle, *Rev. Geophys.* 19 (1981) 394–406.
- [2] D.W. Forsyth, Geophysical constraints on mantle flow and melt generation beneath mid-ocean ridges, in: J. Phipps Morgan, D.K. Blackman, J.M. Sinton (Eds.), *Mantle Flow and Melt Generation at Mid-Ocean Ridges*, Am. Geophys. Union, Washington, DC, 1992, pp. 1–65.
- [3] D.L. Anderson, C.G. Sammis, Partial melting in the upper mantle, *Phys. Earth Planet. Inter.* 3 (1970) 41–50.
- [4] A.E. Ringwood, *Composition and Petrology of the Earth's Mantle*, McGraw-Hill, New York, 1975, 618 pp.
- [5] D.L. Kohlstedt, Structure, rheology and permeability of

- partially molten rocks at low melt fractions, in: J. Phipps Morgan, D.K. Blackman, J.M. Sinton (Eds.), *Mantle Flow and Melt Generation at Mid-Ocean Ridges*, Am. Geophys. Union, Washington, DC, 1992, pp. 102–121.
- [6] H. Schmeling, Numerical model of partial melt on elastic, anelastic and electric properties of rocks, Part I. Elasticity and anelasticity, *Phys. Earth Planet. Inter.* 41 (1985) 34–57.
- [7] H. Sato, I.S. Sacks, T. Murase, G. Muncill, H. Fukuyama, Q_p -melting temperature relation in peridotite at high pressure and temperature: attenuation mechanism and implications for the mechanical properties of the upper mantle, *J. Geophys. Res.* 94 (1989) 10647–10661.
- [8] S. Karato, M.S. Paterson, J.D. Fitz Gerald, Rheology of synthetic olivine aggregates: influence of grain size and water, *J. Geophys. Res.* 91 (1986) 8151–8176.
- [9] S. Karato, The role of hydrogen in the electrical conductivity of the upper mantle, *Nature* 347 (1990) 272–273.
- [10] C.W. Burnham, The importance of volatile constituents, in: J.S. Yoder (Ed.), *The Evolution of the Igneous Rocks*, Princeton University Press, Princeton, NJ, 1979, pp. 439–482.
- [11] D.L. Kohlstedt, H. Keppler, D.C. Rubie, Solubility of water in the α , β and γ phases of $(\text{Mg,Fe})_2\text{SiO}_4$, *Contrib. Mineral. Petrol.* 123 (1996) 345–357.
- [12] S. Karato, Does partial melting reduce the strength of the upper mantle?, *Nature* 319 (1986) 309–310.
- [13] G. Hirth, D.L. Kohlstedt, Water in the oceanic upper mantle: implications for rheology, melt extraction and the evolution of the lithosphere, *Earth Planet. Sci. Lett.* 144 (1996) 93–108.
- [14] J.B. Gaherty, T.H. Jordan, L.S. Gee, Seismic structure of the upper mantle in a central Pacific corridor, *J. Geophys. Res.* 101 (1996) 22291–22309.
- [15] J. Revenaugh, T.H. Jordan, Mantle layering from ScS reverberations, 3. The upper mantle, *J. Geophys. Res.* 96 (1991) 19781–19810.
- [16] S. Karato, Effects of water on seismic wave velocities in the upper mantle, *Proc. Jpn. Acad. B* 70 (1995) 61–66.
- [17] Y. Gueguen, J.-C.-C. Mercier, High attenuation and the low-velocity zone, *Phys. Earth Planet. Inter.* 7, 39–46.
- [18] J.B. Minster, D.L. Anderson, A model of dislocation-controlled rheology for the mantle, *Philos. Trans. R. Soc. London A* 299 (1981) 319–356.
- [19] H.A. Spetzler, D.L. Anderson, The effect of temperature and partial melting on velocity and attenuation in a simple binary mixture, *J. Geophys. Res.* 73 (1968) 6051–6060.
- [20] T. Plank, C.H. Langmuir, Effects of the melting regime on the composition of the oceanic crust, *J. Geophys. Res.* 97 (1992) 19749–19770.
- [21] T. Yoshii, Regionality of group velocities of Rayleigh waves in the Pacific and thickening of the plate, *Earth Planet. Sci. Lett.* 25 (1975) 305–312.
- [22] D.W. Forsyth, The evolution of the upper mantle beneath mid-ocean ridges, *Tectonophysics* 38 (1977) 89–118.
- [23] M. Kumazawa, O.L. Anderson, Elastic moduli, pressure derivatives, and temperature derivatives of single-crystal olivine and single-crystal forsterite, *J. Geophys. Res.* 74 (1969) 5961–5972.
- [24] D.J. Weidner, Elastic properties of rocks and minerals, in: C.G. Sammis, T.L. Heney (Eds.), *Methods of Experimental Physics*, 24A (Geophysics), Academic Press, New York, 1987, pp. 1–30.
- [25] S. Karato, H.A. Spetzler, Defect microdynamics in minerals and solid state mechanisms of seismic wave attenuation and velocity dispersion, *Rev. Geophys.* 28 (1990) 399–421.
- [26] S. Karato, Defects and plastic deformation of olivine, in: S. Karato, M. Toriumi (Eds.), *Rheology of Solids and of the Earth*, Oxford University Press, Oxford, 1989, pp. 176–208.
- [27] D.L. Kohlstedt, B. Evans, S.J. Mackwell, Strength of the lithosphere: constraints imposed by laboratory experiments, *J. Geophys. Res.* 100 (1995) 17587–17602.
- [28] I. Jackson, M.S. Paterson, J.D. FitzGerald, Seismic wave dispersion and attenuation in Aheim dunite: an experimental study, *Geophys. J. Int.* 108 (1992) 517–534.
- [29] E. Ohtani, M. Kumazawa, Melting of forsterite Mg_2SiO_4 up to 15 GPa, *Phys. Earth Planet. Inter.* 27 (1981) 32–38.
- [30] A.M. Dziewonski, D.L. Anderson, Preliminary reference Earth model, *Phys. Earth Planet. Inter.* 25 (1981) 297–356.
- [31] J.-G. Schilling, M.B. Bergeron, R. Evans, Halogens in the mantle beneath the North Atlantic, *Philos. Trans. R. Soc. London A* 297 (1980) 147–178.
- [32] S.J.G. Galer, R.K. O’Nions, Magmagenesis and the mapping of chemical and isotopic variations in the mantle, *Chem. Geol.* 56 (1986) 45–61.
- [33] C.H. Langmuir, E.M. Klein, T. Plack, Petrological systematics of mid-ocean ridge basalts: constraints on melt generation beneath ocean ridges, in: J. Phipps Morgan, D.K. Blackman, J.M. Sinton (Eds.), *Mantle Flow and Melt Generation at Mid-Ocean Ridges*, Am. Geophys. Union, Washington, DC, 1992, pp. 183–280.
- [34] E. Stolper, S. Newman, The role of water in the petrogenesis of Mariana trough magmas, *Earth Planet. Sci. Lett.* 121 (1994) 293–325.
- [35] Y. Bottinga, L. Steinmetz, A geophysical, geochemical, petrological model of the sub-marine lithosphere, *Tectonophysics* 55 (1979) 311–347.
- [36] D.L. Turcotte, G. Schubert, *Geodynamics*, Wiley, New York, 1982.
- [37] D.P. McKenzie, Some remarks on heat flow and gravity anomalies, *J. Geophys. Res.* 72 (1967) 6261–6271.
- [38] D. McKenzie, M.J. Bickle, The volume and composition of melt generated by extension of the lithosphere, *J. Petrol.* 29 (1988) 625–679.
- [39] P.C. Hess, Phase equilibria constraints on the origin of ocean floor basalts, in: J. Phipps Morgan, D.K. Blackman, J.M. Sinton (Eds.), *Mantle Flow and Melt Generation at Mid-Ocean Ridges*, Am. Geophys. Union, Washington, DC, 1992, pp. 67–102.
- [40] M. Olafsson, D.H. Eggler, Phase relations of amphibole, amphibole–carbonate, and phlogopite–carbonate peridotite: petrologic constraints on the asthenosphere, *Earth Planet. Sci. Lett.* 64 (1983) 305–315.
- [41] Y. Shen, D.W. Forsyth, Geochemical constraints on initial

- and final depths of melting beneath mid-ocean ridges, *J. Geophys. Res.* 100 (1995) 2211–2237.
- [42] D.M. Shaw, Trace element fractionation during anatexis, *Geochim. Cosmochim. Acta.* 34 (1970) 237–243.
- [43] D.R. Scott, D.J. Stevenson, A self-consistent model of melting, magma migration and buoyancy-driven circulation beneath mid-ocean ridges, *J. Geophys. Res.* 94 (1989) 2973–2988.
- [44] D.K. Blackman, J.-M. Kendall, P.R. Dawson, H.-R. Wenk, D. Boyce, J. Phipps Morgan, Teleseismic imaging of subaxial flow at mid-ocean ridges: travelttime effects of anisotropic mineral texture in the mantle, *Geophys. J. Int.* 127 (1996) 415–426.
- [45] S. Zhang, S. Karato, Lattice preferred orientation of olivine aggregates deformed in simple shear, *Nature* 375 (1995) 774–777.
- [46] B. Parsons, J.G. Sclater, An analysis of the variation of ocean floor bathymetry and heat flow with age, *J. Geophys. Res.* 82 (1977) 803–827.
- [47] A. Cazanave, B. Parsons, P. Calcagno, Geoid lineations of 1000 km wavelength over the central Pacific, *Geophys. Res. Lett.* 22 (1995) 97–100.
- [48] D.K. Blackman, J.A. Orcott, D.W. Forsyth, J.-M. Kendall, Seismic anisotropy in the mantle beneath an oceanic spreading center, *Nature* 366 (1993) 675–677.
- [49] S. Zhang, M.E. Zimmerman, M.J. Daines, S. Karato, D.L. Kohlstedt, Lattice preferred orientation and melt distribution in experimentally sheared olivine-basalt rocks, *EOS, Trans. Am. Geophys. Union* 76 (1995) 281.
- [50] H.D. Garbin, L. Knopoff, Elastic moduli of a medium with liquid-filled cracks, *Q. Appl. Math.* 33 (1975) 301–301.
- [51] Y. Yu, J. Park, Hunting for azimuthal anisotropy beneath the Pacific ocean region, *J. Geophys. Res.* 99 (1994) 15399–15421.
- [52] T. Tanimoto, D.L. Anderson, Mapping mantle convection, *Geophys. Res. Lett.* 11 (1984) 287–290.
- [53] J.-P. Montagner, T. Tanimoto, Global upper mantle tomography of seismic velocities, *J. Geophys. Res.* 96 (1991) 20337–20351.
- [54] H. Berckhemer, W. Kampfmann, E. Aulbach, H. Schmeling, Shear modulus and Q of forsterite and dunite near partial melting from forced oscillation experiments, *Phys. Earth Planet. Inter.* 29 (1982) 30–41.
- [55] G. Hirth, D.L. Kohlstedt, Experimental constraints on the dynamics of partially molten upper mantle: deformation in the diffusion creep regime, *J. Geophys. Res.* 100 (1995) 1981–2001.